

Parametric Optimization of the Poly (Nvinylcaprolactam) (PNVCL) Thermoresponsive Polymers Synthesis by the Response Surface Methodology and Radial Basis Function neural network

Marwah N. Mohammed^{1,*}, Kamal Bin Yusoh¹, Jun Haslinda Binti Haji Shariffuddin¹

¹ Faculty of Chemical & Natural Resources Engineering, Universiti Malaysia Pahang, 26300, Pahang, Malaysia.

Abstract. . A novel comparison study based on a radial basis function neural network (RBFNN) and Response Surface Methodology (RSM) is proposed to predict the conversion rate (yield) of the experimental data for PNVCL polymerization. A statistical and optimization model was performing to show the effect of each parameter and their interactions on the conversion rate. The influence of the time, polymerization temperature, initiator concentration and concentration of the monomer were studied. The results obtained in this study indicate that the RBFNN was an effective method for predicting the conversion rate. The time of the PNVCL polymerization as well as the concentration of the monomer show the maximum effect on the conversion rate. In addition, compared with the RSM method, the RBFNN showed better conversion rate comparing with the experimental data.

1 Introduction

The recognized thermosensitive polymer with LCST close to physical temperature is Poly (N-vinylcaprolactam) (PNVCL), which is around 32 °C [1]-[3]. For biomedical applications, this type of physiological temperature considered promising especially in drug delivery systems and micro-encapsulation of enzymes or cells [4,5]. Since not long the poly (N-isopropylacrylamide) (PNIPAM) was the most of the environmental thermoresponsive polymer as a homo- and copolymers, but PNVCL has an exceptional advantage make him better than PNIPAM. these remarkable advantage has been proven by cytotoxicity evaluation which proved produce toxic low-molecular-weight amines during hydrolysis [6]. Likewise, there are other features of PNVCL as high complexing ability with different therapeutic agents; low toxicity and biocompatibility make it substantially propose utilized as a hydrophobic core-forming segment with different kinds of hydrophilic moieties at temperatures above its LCST. These features together are widely used in many medical and industrial applications, in special in the biomedical field [7]-[9].

* Corresponding author: marwahnoori85@gmail.com

In manufacturing stage, the two significant issues are process modelling and optimization. For the optimization of process parameters, it is not only excess the product quality but advantage of also the advantage of technologist. Through the manufacturing process to produce polymers a multi-type problem can appear, to identify and summarize these problems the response surface methodology (RSM) utilize to be a simple and effective method of enhancing, analyzing and optimizing the parameter settings [10], [11].

The radical polymerization is the method which is used to synthesise PNVCL starting from the monomer. Although this polymer has a considerable attention the data information on its radical polymerization are rare and significant quantitative characteristics of the reaction are unavailable [12]-[14]. Therefore, the goal of the present study is to investigate the factors which are the effect on synthesis process.

2 Experimental

2.1 Materials and polymerization procedure

N-vinylcaprolactam (98%, provided by Aldrich) as a monomer, 2,20-azobisisobutyronitrile-AIBN (supplied by BASF, Guaratingueta, state of Sao Paulo, Brazil) as initiator, while 1,4-dioxane (99.8%, Aldrich) as a solvent. The PNVCL polymer, was produced by free radical polymerization technique, in 1,4-dioxane at 70 °C for 3 hours, the experimental results were obtained by [15]. The reaction was performed under nitrogen atmosphere, in a double walled glass reactor and heated to reach 70 °C temperatures. At First, the calculated amount of N-vinylcaprolactam was poured in to the reactor, in addition to a suitable volume of internal standard (Trioxane). After the addition of 75% of the 1,4-dioxane, the solution was flushed with argon for almost 20 minutes. A mixed solution of AIBN and the solvent (remaining 25%) was processed and flushed with argon for ~ 20 minutes. When the temperature reached 70 °C, the polymerization was commenced by adding the prepared AIBN solution. The polymerization was carried out for 3 hours at 70 °C.

2.2 Experimental design

Response Surface Methodology (RSM) is a usual experimental design technique for optimization of the chemical engineering processes [16]-[18]. This method is also employed to find out conditions leading to a product with enhanced characteristics or quality [19]-[21]. The present study was aimed to develop the input-output relationships for prediction of the conversion % for PNVCL polymerization. In order to achieve at the most influential variables and its effects a phase parameters were proposed. Response surface methodology (RSM) based on central composite design (CCD) was utilized to develop a model for prediction of the conversion % for PNVCL polymerization from the experimental data. RSM are used to estimate the transfer functions at the optimal region. Hence, CCD approach was selected for the present study. The use of statistical design of experiment (DOE) techniques provides with valuable tools for forecasting the behavior of a system or process [22]-[25].

2.3 RBFNN Optimization Technique

Lowe [26] were a first suggestion the Radial Basis Function neural network (RBFNN), and their interpolation and generalization properties are thoroughly investigated in [26]. RBFNN is an artificial neural network depends on radial basis functions as activation functions; the output of the network is a linear combination of radial basis functions of the inputs and neuron parameters a linear combination of radial basis functions. RBFNN applied on different fields

like a mathematical modelling, pattern classification, approximation of a nonlinear function, control, and time-series prediction. RBFNN able to approximate any reasonable continuous function mapping and reaches a good degree of accuracy [27]-[29]. RBFNN formation from three various layers with feedforward architecture: the input layer, hidden layer (RBFNN), and the output layer. Figure 1 illustrates RBFNN structure.

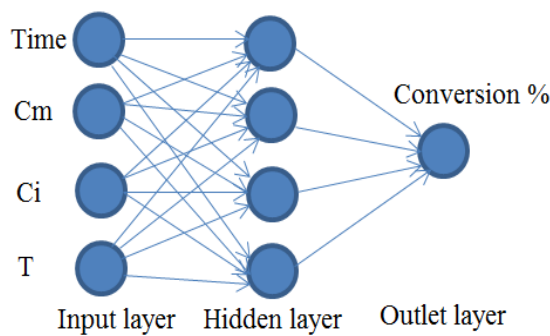


Fig. 1. Radial basis function neural network (RBFNN) structure.

The RBFNN, as a typical feed-forward network, has been found to be very beneficial to many engineering problems [30]. It consists of three layers: the input layer, hidden layer, and output layer. In this study, the activation function ($f(x)$), used as a Gaussian type, and was as follows [31]:

$$\phi(x) = \exp \left[-\frac{\|x - c_i\|^2}{2\sigma_i^2} \right] \tag{1}$$

where, (c_i) and (σ_i) denote the center and spread width of the (i -th) node, respectively, thus ($\|x - c_i\|$) is the Euclidean distance between input vector (x) and center (c_i) [32, 33].

In the current study used MATLAB computer software for optimization. Have been identified (time, Cm, Ci, Temperature) as the inputs of hidden layer (X), and the output conversion % as the output layer (Y) which requires optimizing.

3 Results and Discussion

This research aims to enhance the input and output relationships for prediction of the Conversion rate (yield), the inlet and outlet experimental data for PNVCL polymerization shown in table 1. The analysis of variance (ANOVA) results are presented in Table 2. It can be seen that the model F-value of 26.63 implies the model is significant. There is only a 0.0001% chance that a "Model F-Value" this large could occur due to noise. Values of "Prob > F" less than 0.0500 indicate model terms are significant. In this case Time, Temp. and Time2 are significant model terms. Values greater than 0.1000 indicate the model terms are insignificant. Values greater than 0.1000 indicate the model terms are not significant.

Table 1. Experimental data for PNVCL polymerization [15].

Time (min)	Cm(mol/L)	Ci(mol/L)	T(°C)	Conversion %
45	0.16	0.031	70	78
150	0.16	0.023	60	73
180	0.16	0.023	80	100
150	0.16	0.0235	80	96
20	0.16	0.016	60	21
180	0.16	0.023	60	80
15	0.16	0.031	70	31
45	0.32	0.023	70	71
120	0.32	0.023	70	90
90	0.16	0.023	80	86
45	0.16	0.023	80	69
60	0.32	0.023	70	78
30	0.16	0.023	70	48
150	0.16	0.0235	70	94
90	0.16	0.023	60	50
180	0.32	0.023	70	100
60	0.16	0.023	80	75
30	0.16	0.023	60	27
60	0.16	0.016	70	63
20	0.32	0.023	70	42
90	0.06	0.023	60	61
90	0.16	0.023	70	73
180	0.16	0.016	70	91
90	0.32	0.031	70	87
120	0.16	0.031	70	96
15	0.16	0.016	70	19
90	0.32	0.023	80	88
30	0.06	0.023	70	47
180	0.16	0.031	70	100
120	0.16	0.023	80	93

Table 2. Analysis of variance (ANOVA) results of the yield.

Source	Sum of Squares	df	Mean Square	F value	p-value Prob > F
Model	25146.4	14	1796.17	26.63	< 0.0001 significant
A-Time	12341.9	1	12341.9	182.95	< 0.0001
B-Cm	102.77	1	102.77	1.52	0.2374
C-Ci	132.73	1	132.73	1.97	0.1825
D-Temp	643.16	1	643.16	9.53	0.008
AB	81.1	1	81.1	1.2	0.2914
AC	2.73	1	2.73	0.04	0.8436
AD	25.86	1	25.86	0.38	0.5458
BC	112.3	1	112.3	1.66	0.2179
BD	12.26	1	12.26	0.18	0.6763
CD	102.01	1	102.01	1.51	0.2391
A2	2550.31	1	2550.31	37.81	< 0.0001
B2	20.02	1	20.02	0.3	0.5945
C2	41.82	1	41.82	0.62	0.4442
D2	96.67	1	96.67	1.43	0.2511
Residual	944.43	14	67.46		
Cor Total	26090.8	28			

The mathematical model for the conversion rate (%) is developed based on the response surface method. The mathematical equation of the conversion rate (%) can be expressed as in Eq. (2).

Conversion% = -123.28278 +1.36579*T1 +362.07716*X2
-13759.21200*X3+5.45449*X4
-0.27568*X1*X2-3.44569*X1*X3
-4.79058*10^{^(-3)}*X1*X4-7772.07490*X2*X3
-4.66738*X2*X4+206.38658*X3*X4
-2.75566*10^{^(-3)}*X1^{^2}+470.91392* X2^{^2}
+38677.86803*X3^{^2}-0.054149* X4^{^2};

(2)

The R-Squared analysis result of the conversion rate t is tabulated in Table 3. The Predict R-Squared of 0.9638 is in reasonable agreement with the Adjusted R-Squared of 0.9276. Adequate Precision measures the signal to noise ratio. A ratio greater than 4 is desirable. The ratio of 15.389 indicates an adequate signal. This model can be used to navigate the design space of the meausre the conversion rate. The higher value of R² indicates the better fit of the model with the real data.

Table 3. R2 analysis results of the conversion.

Std. Dev.	8.21	R-Squared	0.9638
Mean	63.62	Adj R-Squared	0.9276
C.V. %	12.91	Pred R-Squared	N/A
PRESS	N/A	Adeq Precision	15.389

The result from RBFNN and DOE was shown in the Table 4. This table highlights the conversion rate for three cases as an experimental, RBFNN predicated and RSM predicated. It was very clear the results from the RBFNN predicated closed to the experimental compared with the RSM predicated data. These results also presented in the Figure 2 to show that the RBFNN predicated results were correspond with experimental data exactly.

Table 4. Result from RBFNN and DOE.

Time (min)	Cm (mol/L)	Ci (mol/L)	T (°C)	Conv. %	RBFNN	DOE	E1	E2
150	0.16	0.023	60	73	73	75.69	0	-2.69
20	0.16	0.016	60	21	21	20.7	0	0.3
15	0.16	0.031	70	31	31	43.4	0	-12.4
120	0.32	0.023	70	90	90	95.69	0	-5.69
45	0.16	0.023	80	69	69	65	0	4
90	0.16	0.023	60	50	50	58.1	0	-8.1
60	0.16	0.016	70	63	63	57.9	0	5.12
180	0.16	0.016	70	91	91	90.25	0	0.74
120	0.16	0.031	70	96	96	96.72	0	-0.72
180	0.16	0.031	70	100	100	99.89	0	0.11

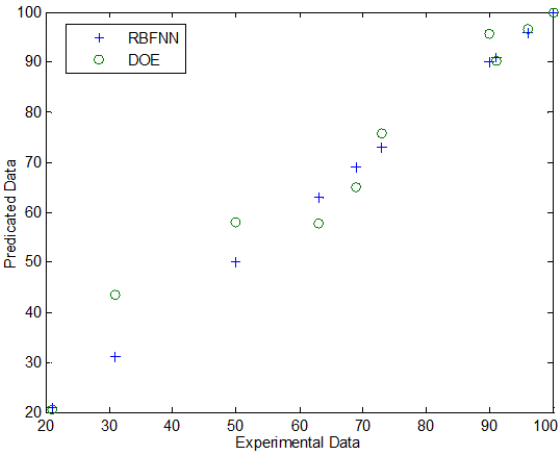


Fig. 2. The best fit line plot of the yield.

4 Conclusion

The application of RSM utilizing a central composite design (CCD) was investigated to elevate the affecting of the polymer conversion by polymerization factor. On the other hand, this study focuses on the predicated data from RBFNN optimization technique. All parameters showed a significant influence on the conversion rate, through ANOVA analysis. The predicted conversion rate show 0% error compared with the experimental results. Therefore, the RBFNN technique represents the more suitable optimization methods to manage the calculations of the conversion rate of the experimental data for the PNVCL polymerization.

References

1. Prabaharan, M., et al., *Macromol. Biosci.*, **8**(9): p. 843-851 (2008).
2. Konefał, R., et al., *Colloid. Polym. Sci.*, p. 1-10 (2016).
3. Yang, Y., et al., *J. Polym. Res.*, **21**(9): p. 1-9 (2014).
4. Loos, W., et al., *Macromol. Chem. Phys.*, **204**(1): p. 98-103 (2003).
5. Verbrugghe, S., K. Bernaerts, and F.E. Du Prez, *Macromol. Chem. Phys.*, **204**(9): p. 1217-1225 (2003).
6. Sun, S. and P. Wu, *J. Phys. Chem. B*, **115**(40): p. 11609-11618 (2011).
7. Hurtgen, M., et al., *J. Polym. Sci. Pol. Chem.*, **50**(2): p. 400-408 (2012).
8. Lequeieu, W., N. Shtanko, and F. Du Prez, *J. Membrane Sci.*, **256**(1): p. 64-71 (2005).
9. Dimitrov, I., et al., *Prog. Polym. Sci.*, **32**(11): p. 1275-1343 (2007).
10. Toloza Porras, C., et al., *Macromol. React. Eng.*, **7**(7): p. 311-326 (2013).
11. Wang, L. and L.J. Broadbelt, *Macromolecules*, **42**(20): p. 7961-7968 (2009).
12. Solomon, O.F., M. Corciovei, and C. Boghin, *J. Appl. Polym. Sci.*, **12**(8): p. 1843-1851 (1968).
13. Solomon, O., D. Vasilescu, and V. Tăărăscu, *J. Appl. Polym. Sci.*, **13**(1): p. 1-7 (1969).
14. Kalugin, D., Y.A. Talyzenkov, and M. Lachinov, *Polym. Sci. Ser. B+*, **50**(11-12): p. 299-304 (2008).
15. Medeiros, S.F., et al., *J. Appl. Polym. Sci.*, **118**(1): p. 229-240 (2010).
16. Jenkins, A.L., M.W. Ellzy, and L.C. Buettner, *J. Mol. Recognit.*, **25**(6): p. 330-335 (2012).
17. Asghari, A., M. Kamalabadi, and H. Farzinia, *Chem. Biochem. Eng. Q.*, **26**(2): p. 145-154 (2012).
18. Madaeni, S. and S. Koocheki, *Chem. Eng. J.*, **119**(1): p. 37-44 (2006).
19. Kaladhar, M., et al., *J. Eng. Sci. Technol. Rev.*, **4**(1): p. 55-61 (2011).
20. Mohamed, A.A., et al., *J. Nucl. R. Technol.*, **9**(1): p. 23-32 (2012).
21. Mehdiinia, A., et al., *J. Chromatogr. A*, **1283**: p. 82-88 (2013).
22. Cui, F., et al., *Biotechnol. Bioproc. E.*, **15**(2): p. 299-307 (2010).
23. San, F.G.B., I. Isik-Gulsac, and O. Okur, *Energy*, **55**: p. 1067-1075 (2013).
24. Khamfroush, M., et al., *Korean J. Chem. Eng.*, **31**(9): p. 1695-1706 (2014).
25. Mirmohseni, A., M. Shojaei, and R. Pourata, *RSC Adv.*, **4**(39): p. 20177-20184 (2014).
26. Lowe, D., *Compl. Syst.*, **2**: p. 321-355 (1988).
27. Wang, S., et al., *Entropy*, **17**(8): p. 5711-5728 (2015).
28. Jiao, G., T. Guo, and Y. Ding, *Water*, **8**(9): p. 367 (2016).
29. Wang, X., et al., *RSC Adv.*, **5**(81): p. 66168-66177 (2015).
30. Rostamizadeh, K., H. Abdollahi, and C. Parsajoo, *Int. Nano Lett.*, **3**(1): p. 1-9 (2013).
31. Erol, R., et al., *J. Med. Syst.*, **32**(3): p. 215-220 (2008).
32. Evans, P., et al., *Sensor. Actuat. B-Chem.*, **69**(3): p. 348-358 (2000).
33. Ghosh-Dastidar, S., H. Adeli, and N. Dadmehr, *IEEE T Bio-Med. Eng.*, **55**(2): p. 512-518 (2008).